Analysis of a Hemispherical Dielectric Resonator Antenna with an Airgap

Kin-Lu Wong, *Member, IEEE*, Nan-Cheng Chen, and Hong-Twu Chen

***Abstract*—A probe-fed hemispherical dielectric resonator antenna with an airgap of hemispherical shape between the dielectric and the ground plane is investigated theoretically by using a Green's function formulation. Input impedance of the efficiently radiating mode of TE_{111} is calculated and analyzed. It is found that, with the presence of the airgap, the antenna bandwidth, obtained from the 3-dB impedance bandwidth, can be considerably enhanced. This study provides a new design for bandwidth enhancement of the dielectric resonator antenna.**

I. Introduction

RECENTLY, it is found that dielectric resonators (DR) of different shapes can be designed to be efficient radiators [1]. A hemispherical DR resting on a ground plane has also been shown to be a good radiator when operated at TE_{111} mode [2], [3]. In this letter, we report a new geometry of a hemispherical DR antenna with an airgap of hemispherical shape between the dielectric and the ground plane, as shown in Fig. 1, to improve the bandwidth of the DR antenna. A similar idea has been successfully applied in a spherical-circular microstrip structure [4], where a significant increase of the half-power bandwidth of the structure is obtained.

In this study, the electric-field Green's function of the antenna fed by a coax is first derived and the input impedance is then formulated by using the reaction formula [3]. Numerical results of the input impedance are presented as a function of the radius of the hemispherical airgap, and the antenna bandwidth, obtained from the 3-dB impedance bandwidth [5], are analyzed. To verify the correctness of the analysis, the results for the case of no airgap presence are also compared with the experimental and theoretical data obtained from other independent work [2], [3]. Effects of different probe lengths and feed positions for such a DR antenna on input resistance are also shown.

II. Theoretical Formulation

The geometry of a hemispherical DR antenna with an airgap of hemispherical shape is shown in Fig. 1. The airgap is with a radius of d, and the region of $d < r < a$ is the DR with a relative permittivity of ϵ_r. A probe of length l and radius r_0 is located at $x = b$. The region of $r > a$ is free space with permittivity ϵ_0 and permeability μ_0. To solve the problem, we first derive the z component of the electric-field Green's function $G_{zz}(\vec{r}.\vec{r}')$ for a z-directed unit source current $\delta(\vec{r} - \vec{r}')\hat{z}'$, where $\vec{r}$ and $\vec{r}'$ represent the field and source coordinates, respectively. Since TE mode is of interest, the Green's function G_{zz} can be expressed in terms of the magnetic Hertz potential $\pi_m\hat{r}$ only [6]. By considering the geometry of Fig. 1 and using the image theory, the function of π_m in each region (air, dielectric, and airgap) can be obtained. Next, by matching boundary conditions at each interface and knowing that $\vec{E} = -\nabla \times (r\pi_m\hat{r})$, the Green's function inside the dielectric region $(d < r < a)$ can be expressed as

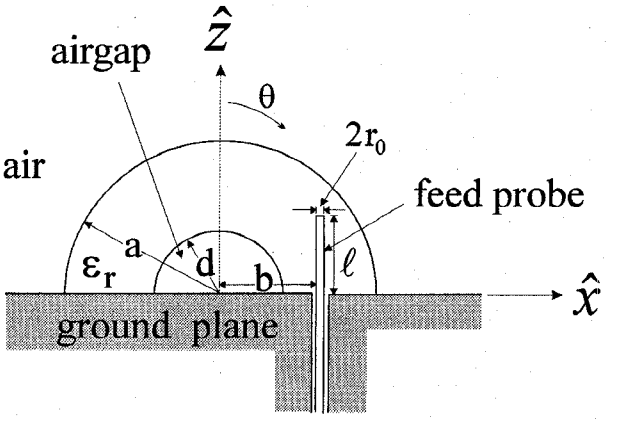

Fig. 1. Geometry of a hemispherical dielectric resonator antenna with an airgap.

$$G_{zz}(\vec{r},\vec{r}') = \frac{-\omega\mu_0}{4\pi}\sum_{n=1}^{\infty}\sum_{m=0}^{n}\left\{\frac{m^2(2n+1)}{n(n+1)}\right.$$
$$\cdot\left[\frac{\hat{J}_n(kr_<)}{kr_<r_>}\hat{H}_n^{(2)}(kr_>) + \frac{b_n}{r}\hat{H}_n^{(2)}(kr) + \frac{c_n}{r}\hat{J}_n(kr)\right]$$
$$\left.\cdot\left[A_{mn}(\theta,\phi,\theta',\phi') + A_{mn}(\theta,\phi,\pi-\theta',\phi')\right]\right\}, \quad (1)$$

Mansucript received May 27, 1993. This work was supported by the National Science Council of the Republic of China under Grant NSC82-0404-E-110-012.

The authors are with the Department of Electrical Engineering, National Sun Yat-Sen University, Kaohsiung, Taiwan 804, Republic of China.

IEEE Log Number 9212460.

where

$$b_n = \frac{\alpha_4\beta_1 - \alpha_2\beta_2}{\alpha_1\alpha_4 - \alpha_2\alpha_3} \text{ and } c_n = \frac{\alpha_1\beta_2 - \alpha_3\beta_1}{\alpha_1\alpha_4 - \alpha_2\alpha_3}, \text{ and}$$

$$\alpha_1 = k_0\hat{H}_n^{(2)\prime}(k_0a)\hat{H}_n^{(2)}(ka) - k\hat{H}_n^{(2)}(k_0a)\hat{H}_n^{(2)\prime}(ka),$$

$$\alpha_2 = k_0\hat{J}_n(ka)\hat{H}_n^{(2)\prime}(k_0a) - k\hat{J}_n'(ka)\hat{H}_n^{(2)}(k_0a),$$

$$\alpha_3 = k_0\hat{J}_n'(kd)\hat{H}_n^{(2)}(kd) - k\hat{J}_n(k_0d)\hat{H}_n^{(2)\prime}(kd),$$

$$\alpha_4 = k_0\hat{J}_n'(k_0d)\hat{J}_n(kd) - k\hat{J}_n(k_0d)\hat{J}_n'(kd),$$

$$\beta_1 = -(\alpha_1/kr')\hat{J}_n(kr'),$$

$$\beta_2 = -(\alpha_4/kr')\hat{H}_n^{(2)\prime}(kr'),$$

$$A_{mn}(\theta,\phi,\theta',\phi') = \xi_m\frac{(n-m)!}{(n+m)!} P_n^m(\cos\theta)P_n^m(\cos\theta')\cos\, m(\phi-\phi'),$$

$$\xi_m = \begin{cases} 1, & m = 0, \\ 2, & m \geq 1, \end{cases}$$

$$k = k_0\sqrt{\varepsilon_r} = \omega\sqrt{\mu_0\varepsilon_0\varepsilon_r}\,.$$

In (1), $r_>$ is the larger of r and r' and $r_<$ is the smaller of r and r' as defined in [7]; $\hat{J}_n(x)$ and $\hat{H}_n^{(2)}(x)$ are, respectively, a spherical Bessel function of the first kind and a spherical Hankel function of the second kind (Shelkunoff type); $P_n^m(x)$ is the associated Legendre function.

Next, by taking the single-mode approximation for TE_{111} mode [3], we have

$$G_{zz}(\vec{r},\vec{r}') = \frac{-3\omega\mu_0}{4\pi}\sin\theta'\sin\theta\cos(\phi-\phi')$$
$$\begin{cases} \frac{1}{krr'}\hat{J}_1(kr')\hat{H}_1^{(2)}(kr) + \frac{b_1}{r}\hat{H}_1^{(2)}(kr) + \frac{c_1}{r}\hat{J}_1(kr), & r > r', \\ \frac{1}{krr'}\hat{J}_1(kr)\hat{H}_1^{(2)}(kr') + \frac{b_1}{r}\hat{H}_1^{(2)}(kr) + \frac{c_1}{r}\hat{J}_1(kr), & r < r'. \end{cases} \tag{2}$$

Using (2), the electric field E_z due to a probe surface current J_z can be expressed as

$$\vec{E}_z(\vec{r}) = \int\int_{S_0} G_{zz}(\vec{r},\vec{r}')\vec{J}_z(z')\,ds', \qquad S_0 : \text{ source surface} \tag{3}$$

and the input impedance is then determined by

$$Z_{in} = \frac{-1}{I_z^2(0)}\int\int_{S_0} E_z(\vec{r})J_z(z)\,dS. \tag{4}$$

III. Numerical Results and Discussion

In this section, typical numerical results of the input impedance at TE_{111} mode are presented. The effects of introducing an airgap into the hemispherical DR antenna are first discussed in Fig. 2, where the input impedance for the antenna with different radii of the hemispherical airgap is shown. To confirm the correctness of the numerical results presented here, the data obtained in [2],[3] for the case of no airgap presence (i.e., $d = 0$) are also shown in the figure for comparison. It is clearly seen that our input resistance results of $d = 0$ in Fig. 2(a) agree well with the data obtained in [2], [3]. As for the input reactance curve, our result shown in Fig. 2(b) is also in good agreement with the theoretical data in [3] and

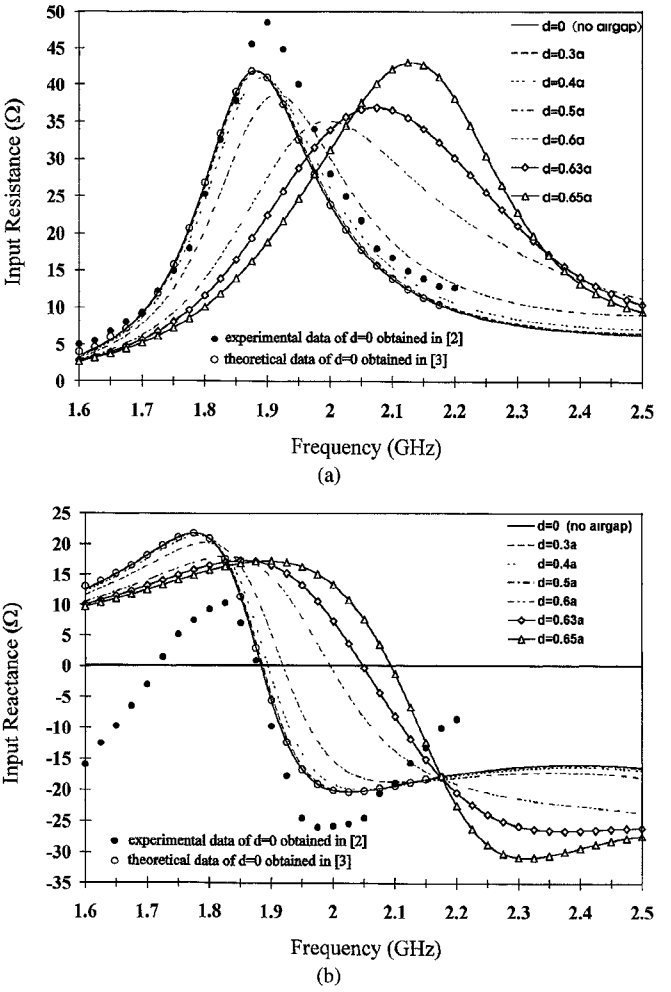

Fig. 2. (a) Input resistance and (b) input reactance of a hemispherical dielectric resonator antenna with a=2.54cm, b=1.74cm, l=1.52cm, r_0=0.075cm, ε_r=8.9. The solid and open circles denote, respectively, the experimental data in [2] and the theoretical data in [3] for the case of no airgap presence.

the measured data around resonance [2]. This can ascertain the correctness of the numerical calculation here. From the results, it is found that, for d less than 0.3a, the effects of the airgap on the input impedance is negligible. For $d > 0.3a$, the resonant frequency shifts to higher frequencies, and the resonant input resistance is gradually decreased until reaching a minimum value of about 35Ω at $d = 0.6a$. Fig. 3 shows the variation of the bandwidth, obtained from the 3-dB impedance bandwidth [5], with the airgap radius d. It is seen that, with the presence of the airgap, the antenna bandwidth increases and reaches a maximum value of about 24% at $d = 0.6a$, which is nearly two times of that for no airgap presence.

Variations of input resistance at resonance with feed position for different probe lengths are also studied. The results are shown in Fig. 4, where two cases of $d = 0$ (no airgap) and $d = 0.4a$ (with an airgap) are presented. The open circles in the figure are the data obtained in [3] for $d = 0$. Again, good agreement with the results calculated here is observed. From the results in Fig. 4, it is clear that for both cases the input resistance increases until reaching a maximum value, as the probe moves away from the center. This behavior is useful for impedance matching. Finally, it should be noted

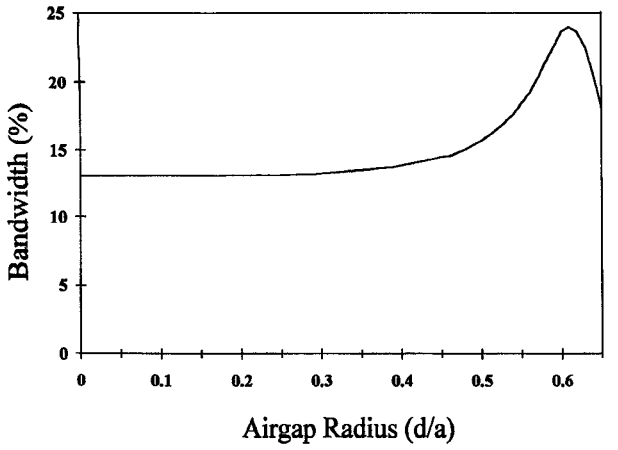

Fig. 3. Variation of the bandwidth with the airgap radius d. The antenna parameters are the same as in Fig. 2.

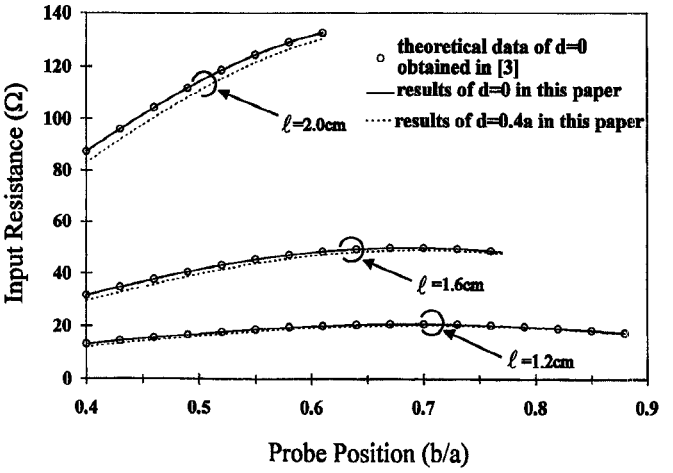

Fig. 4. Input resistance at resonance versus feed position for different probe lengths; $a = 2.54$ cm, $b = 1.74$ cm, $r_0 = 0.075$ cm, $d = 0$ (no airgap) and $0.4a$ (with an airgap). The open circles are the theoretical data obtained in [3] for the case of no airgap presence.

that since the proposed configuration in Fig. 1 is just like a hollow hemispherical DR structure resting on a ground plane, the implementation of this new geometry will be easy. Additional results obtained by calculating the far-zone radiated fields (not shown here) also indicate that the airgap does not alter the radiation pattern of the hemispherical DR antenna at TE_{111}mode, whose maximum radiation is normal to the ground plane.

IV. Conclusion

A new geometry of a hemispherical DR antenna with an airgap of hemispherical shape is studied. Numerical results of the input impedance at TE_{111} mode are presented. Results indicate that the antenna bandwidth can be considerably increased by introducing an optimal size of the airgap into the DR antenna. For the antenna parameters studied here, when the airgap radius is about $0.6a$, the antenna bandwidth can reach about 24%, nearly two times of that for no airgap presence. Furthermore, for such a geometry impedance matching can also be achieved by adjusting the probe length and feed position.

References

[1] S. A. Long, M. W. McAllister, and L. C. Shen, "The resonant cylindrical dielectric cavity antenna," *IEEE Trans. Antennas Propagat.*, vol. AP-31, pp. 406–412, 1983.

[2] M. W. McAllister and S. A. Long, "Resonant hemispherical dielectric antenna," *Electron. Lett.*, vol. 20, pp. 657–659, 1984.

[3] K. W. Leung, K. M. Luk, K. Y. A. Lai, and D. Lin, "Input impedance of hemispherical dielectric resonator antenna," *Electron. Lett.*, vol. 27, pp. 2259–2260, 1991.

[4] K. L. Wong and H. T. Chen, "Resonance in a spherical-circular microstrip structure with an airgap," *IEEE Trans. Microwave Theory Tech.*, vol. 41, Aug. 1993. (in press)

[5] T. M. Au and K. M. Luk, "Effects of parasitic element on the characteristics of microstrip antenna," *IEEE Trans. Antennas Propagat.*, vol. 39, pp. 1247–1251, 1991.

[6] R. F. Harrington, *Time-Harmonic Electromagnetic Fields.* New York: McGraw-Hill, 1961, pp. 267–269.

[7] W. C. Chew, *Waves and Fields in Inhomogeneous Media.* New York: Van Nostrand Reinhold, 1990, p. 193.